

PAPER • OPEN ACCESS

## Periodic response of an axially high-speed moving beam under 3:1 internal resonance

To cite this article: Hu Ding *et al* 2016 *J. Phys.: Conf. Ser.* **744** 012117

View the [article online](#) for updates and enhancements.

You may also like

- [Force driven nonlinear vibrations of a thin plate with 1:1:1 internal resonance in a fractional viscoelastic medium](#)  
M V Shitikova and V V Kandu
- [Nonlinear vibration of iced cable under wind excitation using three-degree-of-freedom model](#)  
Wei Zhang, , Ming-Yuan Li et al.
- [Research on Time Delay Feedback Control of Lateral Vibration Axially Moving Viscoelastic Beam](#)  
Bo Wang and Youqi Tang



**ECS**  
The  
Electrochemical  
Society  
Advancing solid state &  
electrochemical science & technology

**DISCOVER**  
how sustainability  
intersects with  
electrochemistry & solid  
state science research

# Periodic response of an axially high-speed moving beam under 3:1 internal resonance

Hu Ding<sup>1</sup>, Xiao-Ye Mao<sup>1</sup> and Li-Qun Chen<sup>1,2</sup>

<sup>1</sup> Shanghai Institute of Applied Mathematics and Mechanics, Shanghai University, Shanghai 200072, China

<sup>2</sup> Department of Mechanics, Shanghai University, Shanghai 200444, China

Corresponding author's E-mail address: dinghu3@shu.edu.cn (H. Ding)

**Abstract.** In the supercritical speed range, nonlinear forced vibration of an axially moving viscoelastic beam in the presence of 3:1 internal resonance is investigated. The straight beam becomes buckled due to the supercritical moving speed. The governing equation is cast for motion around buckled configuration by using a coordinate transform. Moreover, the first two modes of the buckled beam are set to 3:1 by adjusting the axial moving speed. Then the corresponding equation is approximately analyzed by utilizing the multi-scale method. For the beam subjected to the primary resonances and super-harmonic resonance with internal resonance, frequency-amplitude relationship of steady-state responses is constructed. Numerical examples discovered the influence of internal resonance on the nonlinear dynamic characteristics of the axially moving beam. Specifically, the energy transfer between the first two order modes is found for an axially supercritical moving beam. Moreover, several typical nonlinear phenomenon, such as double jumping phenomenon, hysteretic phenomenon and saturation-like phenomenon, are discovered in the nonlinear vibration of the axially moving beam. By comparing with numerically simulative results via the finite difference method and the Galerkin method, it is confirmed that the method of multi-scale in the present work is quite credible.

## 1. Introduction

Model of axially moving continuums demonstrate so many devices which used after the first industrial revolution. The most typical device is belt-drive dynamics system. It is light, high efficient, and it is easy to design. However, the translating belt will vibration fiercely in some certain conditions. The vibration usually brings strong noise and reduces the service life of these devices. If the mechanism of the vibration is fully understood, the vibration is avoided or reduced during the design progress. Therefore, many researchers have paid their attention to the dynamics of axially moving continuums, specially axially moving beams. Moreover, many interesting phenomenon and meritorious conclusions have been found [1-4].

As it is well-known, the internal resonance of the axially moving beam occur in certain conditions. By this moment, there is a commensurable relationship among the natural frequencies. Under the internal resonance condition, the nonlinear vibration of the beams become much more complex. Therefore, many researchers paid their attentions on the internal resonance of axially moving systems. By using the method of multiple scales Riedel and Tan researched the forced vibration of moving strip with 3:1 internal resonance [5]. Sze *et al.* investigated the forced response of an moving strip with internal resonance between the first two transverse vibration modes [6,7]. Ghayesh and his co-workers

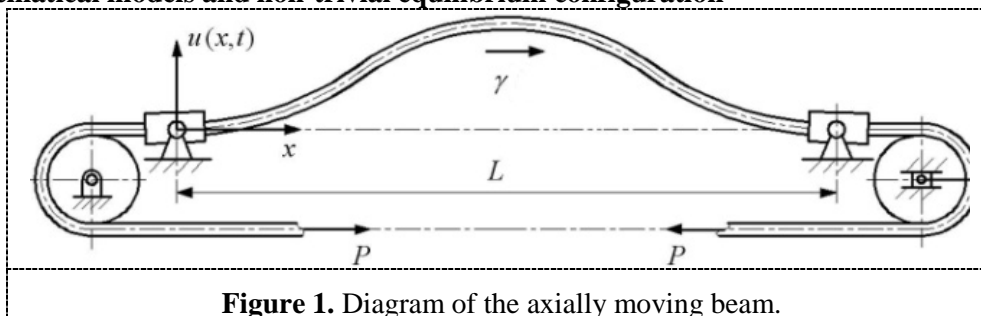


made their contributions on the nonlinear vibration of the moving beams with the internal resonance. The transverse vibration [8], coupled longitudinal-transverse vibration [9], the nonlinear vibration of the Timoshenko beam [10] are studied by them. Tang *et al.* are analytically and numerically investigated the parametric resonance with 3:1 internal resonance of axially moving viscoelastic beams on elastic foundation [11]. Sahoo *et al.* analyzed the nonlinear transverse vibration of an axially moving beam subject to two frequency excitation, i.e. principal parametric resonance of first mode and combination parametric resonance, in presence of internal resonance [12].

However, all of above literatures only focused on nonlinear vibration of axially moving beams with the internal resonance in the subcritical speed range. On the other hand, Wickert worked on the non-trivial equilibrium configuration of a supercritically moving beam [13]. Ding and his co-workers focused their attentions on the vibration of the supercritically axially moving beam, such as natural frequencies [14] and nonlinear forced transverse vibrations [15]. However, the nonlinear dynamics of a axially moving beam with the internal resonance in the supercritical regime hasn't drawn enough attentions. Ghayesh *et al.* numerically investigated the global dynamics of an axially moving beam subjected to a transverse harmonic excitation force with a three-to-one internal resonance.

The present work analytically and numerically studies the steady-state responses of a axially moving viscoelastic beam in the supercritical speed range with the 3:1 internal resonance. The steady-state responses of the primary resonances and super-harmonic resonance with internal resonance are detailedly investigated.

**2. Mathematical models and non-trivial equilibrium configuration**



As shown in figure 1, an axially moving beam with cross-sectional area  $A$ , density  $\rho$ , viscoelastic coefficient  $\Lambda$ , initial tension  $P$ , moment of inertial  $I$  and Young's modulus  $E$ , travels at the uniform constant transport speed  $V$ . The distance between the two simply supported ends is  $L$  and the excitation of the extraneous harmonic force  $F$  is written as  $B\cos(\Omega t)$ . The symbols  $B$  and  $\Omega$  are the amplitude and the frequency, respectively.

The governing equation of the transverse vibration of the moving beam and the simply supported boundary conditions are obtained as follows

$$\rho A \left( W_{,TT} + 2W_{,TX} V + V^2 W_{,XX} \right) + M_{,XX} - P W_{,XX} - \frac{A}{L} W_{,XX} \int_0^L \sigma dX = F$$

$$\sigma = \left( E + \Lambda \frac{d}{dt} \right) \varepsilon_X, M = \left( EI + \Lambda I \frac{d}{dt} \right) W_{,XX}, \tag{1}$$

$$W(0,T) = W(L,T) = 0, W_{,XX}(0,T) = W_{,XX}(L,T) = 0$$

where  $W(X,T)$  is the vertical displacement of the moving beam, and the comma preceding  $T$  or  $X$  denotes partial differentiation with respect to  $T$  or  $X$ . To cast governing equations and boundary conditions dimensionless, the dimensionless variables and the dimensionless parameters are introduced as below

$$w = \frac{W}{L}, x = \frac{X}{L}, t = \frac{T}{L} \sqrt{\frac{P}{\rho A}}, \gamma = V \sqrt{\frac{\rho A}{P}}, b = \frac{BL}{P}, \omega = \Omega L \sqrt{\frac{\rho A}{P}}, \alpha = \frac{I\Lambda}{L^3 \sqrt{\rho AP}}, k_1^2 = \frac{EA}{P}, k_f^2 = \frac{EI}{PL^2} \quad (2)$$

Therefore, dimensionless governing equations and boundary conditions are led as

$$w_{,tt} + 2\gamma w_{,xt} + (\gamma^2 - 1)w_{,xx} + k_f^2 w_{,xxxx} + \alpha w_{,xxxxt} = \frac{k_1^2}{2} w_{,xx} \int_0^1 w_{,x}^2 dx + \frac{\alpha k_1^2}{k_f^2} w_{,xx} \int_0^1 w_{,x} w_{,xt} dx + b \cos(\omega t), \quad (3)$$

$$w(0,t) = w(1,t) = 0, w_{,xx}(0,t) = w_{,xx}(1,t) = 0$$

In the supercritical regime, the non-trivial equilibrium configurations are defined as

$$\hat{w}(x) = \pm \frac{2}{kk_1\pi} \sqrt{\gamma^2 - 1 - k_f^2 k^2 \pi^2} \sin(k\pi x), (k = 1, 2, 3 \dots) \quad (4)$$

Therefore, the governing equation of the supercritically axially moving beam is derived

$$w_{,tt} + 2\gamma w_{,xt} + (\gamma^2 - 1)w_{,xx} + k_f^2 w_{,xxxx} + \alpha w_{,xxxxt} = \frac{k_1^2}{2} (w_{,xx} + \hat{w}_{,xx}) \int_0^1 (w_{,x} + \hat{w}_{,x})^2 dx + \frac{\alpha k_1^2}{k_f^2} (w_{,xx} + \hat{w}_{,xx}) \int_0^1 (w_{,x} + \hat{w}_{,x}) w_{,xt} dx - \frac{k_1^2}{2} \hat{w}_{,xx} \int_0^1 \hat{w}_{,x}^2 dx + b \cos(\omega t) \quad (5)$$

The first four natural frequencies are calculated by using Galerkin method [14]. Furthermore, natural frequencies and 3:1 internal resonance condition between the first-two order modes are determined. If the dimensionless axially moving speed equal to 4.02795, the first frequency equal to 10 and the second one equal to 30.

### 3. Galerkin truncation & multi-scale method for the primary resonance

In order to solve the governing equation (5), the Galerkin method is applied in this work. Suppose the solution of Eq. (5) as

$$w(x,t) = \sum_{i=1}^k q_i(t) \sin(i\pi x), i = 1, 2, \dots, k \quad (6)$$

where  $q_i(t)$  is the  $k$ th modal coordinate of the axially moving beam. The set of ordinary differential equations are derived

$$\mathbf{M}\ddot{\mathbf{q}} + \mathbf{C}\dot{\mathbf{q}} + \mathbf{R}_{(1)}\dot{\mathbf{q}} + \mathbf{R}_{(2)} + \mathbf{R}_{(3)}\mathbf{q} + \mathbf{K}_{(1)}\mathbf{q} + \mathbf{K}_{(2)} + \mathbf{K}_{(3)}\mathbf{q} = \mathbf{F} \quad (7)$$

where  $\mathbf{M}$  is a  $k \times k$  order identity mass matrix,  $\mathbf{C}$  is a  $k \times k$  order inertia coefficient matrix,  $\mathbf{R}_{(1)}$  is a  $k \times k$  order linear viscous damping coefficient matrix,  $\mathbf{R}_{(2)}$  is a  $k$ -order quadratic nonlinear damping force column vector,  $\mathbf{R}_{(3)}$  is a  $k \times k$  order diagonal cubic nonlinear viscous damping coefficient matrix,  $\mathbf{K}_{(1)}$  is a  $k \times k$  order diagonal linear stiffness matrix,  $\mathbf{K}_{(2)}$  is a  $k$ -order quadratic nonlinear elastic restoring force column vector,  $\mathbf{K}_{(3)}$  is a  $k \times k$  order diagonal cubic nonlinear stiffness matrix,  $\mathbf{F}$  is a  $k$ -order exciting force column vector.

The steady-state responses of the moving beam are investigated by using the multi-scale method. The expansion of the perturbation solution is written as follows

$$\mathbf{q} = \mathbf{q}_0 + \varepsilon \mathbf{q}_1 + \varepsilon^2 \mathbf{q}_2 \quad (8)$$

where  $T_0=t, T_1=\varepsilon t, T_2=\varepsilon^2 t$ . Therefore,

It follows that the derivatives with respect to  $t$  become expansions in terms of the partial derivatives with respect to the time scales  $T_n$  according to

$$\frac{d}{dt} = \frac{dT_0}{dt} \frac{\partial}{\partial T_0} + \frac{dT_1}{dt} \frac{\partial}{\partial T_1} + \dots = D_0 + \varepsilon D_1 + \dots, \frac{d^2}{dt^2} = D_0^2 + 2\varepsilon D_0 D_1 + \varepsilon^2 (D_1^2 + 2D_0 D_2) + \dots \quad (9)$$

Furthermore, the forcing and damping are scaled as

$$q_k \leftrightarrow \varepsilon q_k, \alpha \leftrightarrow \varepsilon^2 \alpha, b \leftrightarrow \varepsilon^3 b \tag{10}$$

The part of work in this study is the research to the primary response under the condition of 3:1 internal resonance between the first two order natural frequencies. The 4th-order discrete functions of the moving beam system is written as follows

$$\begin{aligned} \ddot{q}_1 - \mu_1 \dot{q}_2 - \mu_2 \dot{q}_4 + k_{11} q_1 &= bh \cos(\omega t) - \alpha \alpha_{13} \dot{q}_1 \\ &- \alpha \alpha_{14} (2q_1 \dot{q}_1 + 4q_2 \dot{q}_2 + 9q_3 \dot{q}_3 + 16q_4 \dot{q}_4) - \alpha_{11} (3q_1^2 + 4q_2^2 + 9q_3^2 + 16q_4^2) \\ &- \alpha \alpha_{15} q_1 (q_1 \dot{q}_1 + 4q_2 \dot{q}_2 + 9q_3 \dot{q}_3 + 16q_4 \dot{q}_4) - \alpha_{12} q_1 (q_1^2 + 4q_2^2 + 9q_3^2 + 16q_4^2), \\ \ddot{q}_2 + \mu_1 \dot{q}_1 - \mu_3 \dot{q}_3 + k_{21} q_2 &= -4\alpha \alpha_{23} \dot{q}_2 - 4\alpha \alpha_{14} \dot{q}_1 q_2 \\ &- 4\alpha \alpha_{15} q_2 (q_1 \dot{q}_1 + 4q_2 \dot{q}_2 + 9q_3 \dot{q}_3 + 16q_4 \dot{q}_4) - 8\alpha_{11} q_1 q_2 - 4\alpha_{12} q_2 (q_1^2 + 4q_2^2 + 9q_3^2 + 16q_4^2), \\ \ddot{q}_3 + \mu_3 \dot{q}_2 - \mu_4 \dot{q}_4 + k_{31} q_3 &= \frac{1}{3} bh \cos(\omega t) - 9\alpha \alpha_{33} \dot{q}_3 \\ &- 9\alpha \alpha_{14} \dot{q}_1 q_3 - 9\alpha \alpha_{15} q_3 (q_1 \dot{q}_1 + 4q_2 \dot{q}_2 + 9q_3 \dot{q}_3 + 16q_4 \dot{q}_4) \\ &- 18\alpha_{11} q_1 q_3 - 9\alpha_{12} q_3 (q_1^2 + 4q_2^2 + 9q_3^2 + 16q_4^2), \\ \ddot{q}_4 + \mu_4 \dot{q}_3 + \mu_2 \dot{q}_1 + k_{41} q_4 &= -16\alpha \alpha_{43} \dot{q}_4 - 16\alpha \alpha_{14} \dot{q}_1 q_4 \\ &- 16\alpha \alpha_{15} q_4 (q_1 \dot{q}_1 + 4q_2 \dot{q}_2 + 9q_3 \dot{q}_3 + 16q_4 \dot{q}_4) - 32\alpha_{11} q_1 q_4 - 16\alpha_{12} q_4 (q_1^2 + 4q_2^2 + 9q_3^2 + 16q_4^2) \end{aligned} \tag{11}$$

where

$$\begin{aligned} \mu_1 &= \frac{16}{3} \gamma, \quad \mu_2 = \frac{32}{15} \gamma, \quad \mu_3 = \frac{48}{5} \gamma, \quad \mu_4 = \frac{96}{7} \gamma, \\ k_{11} &= \frac{1}{2} k_1^2 \pi^4 A_s^2, k_{21} = 12\pi^4 k_f^2, k_{31} = 72k_f^2 \pi^4, k_{41} = 240k_f^2 \pi^4, \quad \alpha_{11} = \frac{1}{4} k_1^2 \pi^4 A_s, \alpha_{12} = \frac{1}{4} k_1^2 \pi^4, \\ \alpha_{13} &= \left( \frac{k_1^2 A_s^2}{2k_f^2} + 1 \right) \pi^4, \alpha_{23} = 4\pi^4, \alpha_{33} = 9\pi^4, \alpha_{43} = 16\pi^4, \alpha_{14} = \frac{\pi^4 k_1^2 A_s}{2k_f^2}, \alpha_{15} = \frac{\pi^4 k_1^2}{2k_f^2}, \quad h = \frac{4}{\pi} \end{aligned} \tag{12}$$

The V-belt derive systems are widely used today. Moreover, the belt is usually simplified as an axially moving beam. Table 1 shows the physical parameters of the V-belt. Therefore,  $k_1=40$ ,  $k_f=0.8$ . Moreover, set  $b=0.5$  and  $\alpha=0.0001$ .

**Table 1.** Physical parameters of a V-belt transmission.

Item	Notation	Value
Cross-section area	$A$	$5.671 \times 10^{-5} \text{ m}^2$
Moment of inertial	$I$	$2.775 \times 10^{-9} \text{ m}^4$
Initial tension	$P$	7 N
Length of the belt	$L$	0.35 m
Young's modulus	$E$	200 MPa

Instead of using the frequency of excitation  $\Omega$  as a parameter,  $\sigma_1$  and  $\sigma_2$  are introduced as

$$\omega_2 = 3\omega_1 + \varepsilon^2 \sigma_1, \quad \omega = \omega_1 + \varepsilon^2 \sigma_2 \tag{13}$$

The approximate analytical solutions of the primary resonance is determined by using the multi-scale method. Figure 2 shows the variation tendency of the response of  $q_1$  at the first order mode

changing with the excitation frequency.  $a_1$  and  $a_2$  here are the responses of natural modes respectively. As can be seen from figure 3, the curve is bended to the decreasing direction of the excitation frequency nears the external resonance. Therefore, the nonlinear characteristic is soft, although the system contains the cubic nonlinear restoring force. The analytical approximate solutions are compared with numerical simulations to confirm the accuracy of analytical results. All the numerical simulations in this paper are obtained by a set of four-order Galerkin truncated functions. Moreover, the simulation results are calculated by the 4th Runge-Kutta method. Compared with the simulation results, the analysis results are accurate. The dash line is on behalf of the unstable boundary.

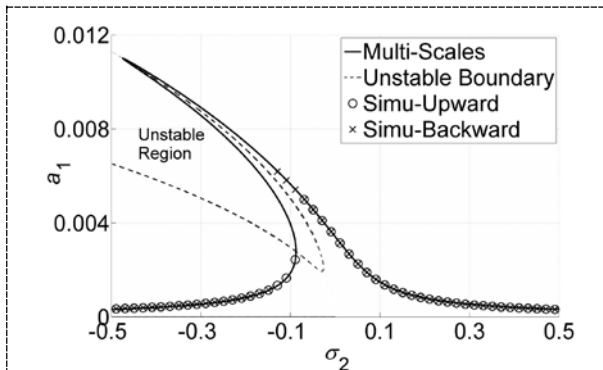


Figure 2. A-F curve of  $q_1$  at the first-order mode.

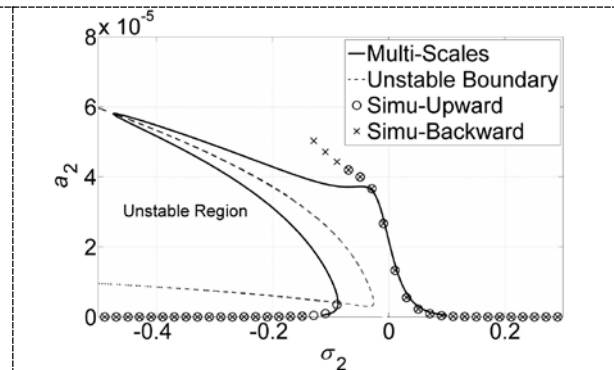


Figure 3. A-F curve of  $q_1$  at the second-order mode.

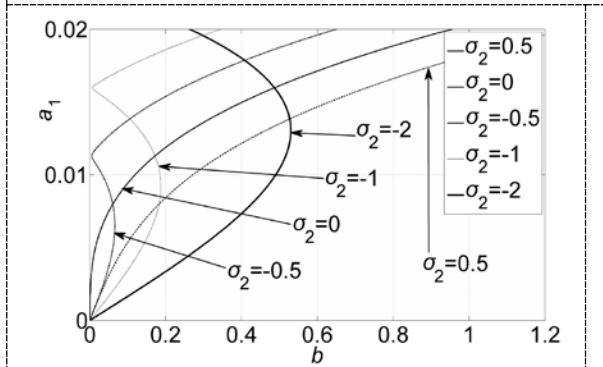


Figure 4. A-b curve of  $q_1$  at the first-order mode

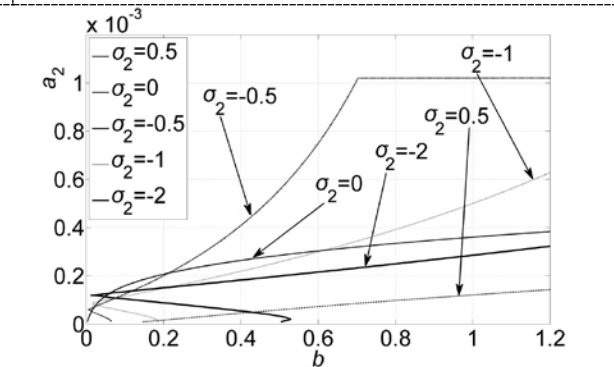
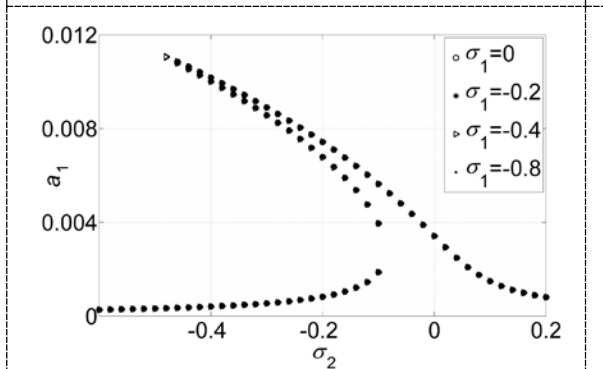
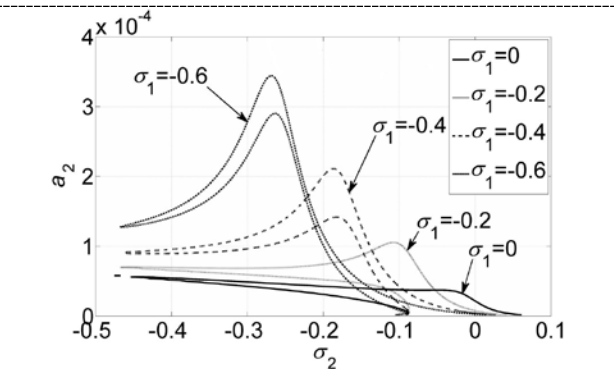


Figure 5. A-b curve of  $q_1$  at the second-order mode



(a) response of the first-order mode



(b) response of the second-order mode

Figure 6. Effect of detuning parameter  $\sigma_1$

Figures 4 and 5 show the hysteresis phenomenon, the typical phenomenon of a nonlinear system, of the axially moving beam under forced and internal resonances. As the nonlinear character is soft, the hysteresis phenomenon occurs only while  $\sigma_2$  is negative. One thing should be particularly

revelatory is the saturated phenomenon in figure 5. The interesting phenomenon occurs at the first order primary resonance. Figure 6 is the responses of  $a_1$  and  $a_2$  with different  $\sigma_1$ . As can be seen from the left figure,  $a_1$  changes very little. But the response at the second mode will increase as the detuning parameter is decreasing.

**4. Super-harmonic resonance by using the directly multi-scale method**

Substitution of  $T_0=t, T_1=\varepsilon t, T_2=\varepsilon^2 t.$  into  $w(x, t)$  deduces following operators

$$\begin{aligned}
 w(x, t) &= w(x, T_0, T_1, T_2); \\
 \frac{\partial}{\partial t} w(x, t) &= \frac{\partial}{\partial T_0} w(x, T_0, T_1, T_2) + \varepsilon \frac{\partial}{\partial T_1} w(x, T_0, T_1, T_2) + \varepsilon^2 \frac{\partial}{\partial T_2} w(x, T_0, T_1, T_2); \\
 \frac{\partial^2}{\partial t^2} w(x, t) &= \frac{\partial^2}{\partial T_0^2} w(x, T_0, T_1, T_2) + \varepsilon \frac{\partial^2}{\partial T_1 \partial T_0} w(x, T_0, T_1, T_2) + \varepsilon^2 \frac{\partial^2}{\partial T_2 \partial T_0} w(x, T_0, T_1, T_2) \\
 &+ \varepsilon \left[ \frac{\partial^2}{\partial T_1 \partial T_0} w(x, T_0, T_1, T_2) + \varepsilon \frac{\partial^2}{\partial T_1^2} w(x, T_0, T_1, T_2) + \varepsilon^2 \frac{\partial^2}{\partial T_2 \partial T_1} w(x, T_0, T_1, T_2) \right] \\
 &+ \varepsilon^2 \left[ \frac{\partial^2}{\partial T_2 \partial T_0} w(x, T_0, T_1, T_2) + \varepsilon \frac{\partial^2}{\partial T_2 \partial T_1} w(x, T_0, T_1, T_2) + \varepsilon^2 \frac{\partial^2}{\partial T_2^2} w(x, T_0, T_1, T_2) \right]
 \end{aligned} \tag{14}$$

The approximate solution of  $w(x, t)$  is written as

$$w(x, T_0, T_1, T_2) = w_0(x, T_0, T_1, T_2) + \varepsilon w_1(x, T_0, T_1, T_2) + \varepsilon^2 w_2(x, T_0, T_1, T_2) \tag{15}$$

Equate the coefficients of  $\varepsilon^0, \varepsilon^1$  and  $\varepsilon^2$  of both sides, three functions are derived as

$$\begin{aligned}
 &\frac{\partial^2}{\partial T_0^2} w_0 + 2\gamma \frac{\partial^2}{\partial T_0 \partial x} w_0 + k_f^2 \pi^2 \frac{\partial^2}{\partial x^2} w_0 + k_f^2 \frac{\partial^4}{\partial x^4} w_0 \\
 &+ 4\pi(\gamma^2 - 1 - k_f^2 \pi^2) \sin(\pi x) \int_0^1 \cos(\pi x) \frac{\partial}{\partial x} w_0 \, dx = b \cos(\Omega T_0)
 \end{aligned} \tag{16}$$

$$\begin{aligned}
 &\frac{\partial^2}{\partial T_0^2} w_1 + 2\gamma \frac{\partial^2}{\partial T_0 \partial x} w_1 + k_f^2 \pi^2 \frac{\partial^2}{\partial x^2} w_1 + k_f^2 \frac{\partial^4}{\partial x^4} w_1 + 2\gamma \frac{\partial^2}{\partial T_1 \partial x} w_0 + 2 \frac{\partial^2}{\partial T_1 \partial T_0} w_0 \\
 &- 2k_1 \frac{\partial^2}{\partial x^2} w_0 \sqrt{\gamma^2 - 1 - k_f^2 \pi^2} \int_0^1 \cos(\pi x) \frac{\partial}{\partial x} w_0 \, dx + 4\pi(\gamma^2 - 1 - k_f^2 \pi^2) \sin(\pi x) \int_0^1 \cos(\pi x) \frac{\partial}{\partial x} w_1 \, dx \\
 &+ k_1 \pi \sqrt{\gamma^2 - 1 - k_f^2 \pi^2} \sin(\pi x) \int_0^1 \left( \frac{\partial}{\partial x} w_0 \right)^2 \, dx = 0
 \end{aligned} \tag{17}$$

$$\begin{aligned}
 &\frac{\partial^2}{\partial T_0^2} w_2 + 2\gamma \frac{\partial^2}{\partial T_0 \partial x} w_2 + k_f^2 \pi^2 \frac{\partial^2}{\partial x^2} w_2 + k_f^2 \frac{\partial^4}{\partial x^4} w_2 + 4\pi(\gamma^2 - 1 - k_f^2 \pi^2) \sin(\pi x) \int_0^1 \cos(\pi x) \frac{\partial}{\partial x} w_2 \, dx \\
 &- 2k_1 \frac{\partial^2}{\partial x^2} w_0 \sqrt{\gamma^2 - 1 - k_f^2 \pi^2} \int_0^1 \cos(\pi x) \frac{\partial}{\partial x} w_1 \, dx + 2k_1 \pi \sqrt{\gamma^2 - 1 - k_f^2 \pi^2} \sin(\pi x) \int_0^1 \left( \frac{\partial}{\partial x} w_0 \right) \left( \frac{\partial}{\partial x} w_1 \right) \, dx \\
 &- 2k_1 \frac{\partial^2}{\partial x^2} w_1 \sqrt{\gamma^2 - 1 - k_f^2 \pi^2} \int_0^1 \cos(\pi x) \frac{\partial}{\partial x} w_0 \, dx - \frac{1}{2} k_1^2 \frac{\partial^2}{\partial x^2} w_0 \int_0^1 \left( \frac{\partial}{\partial x} w_0 \right)^2 \, dx + \alpha \frac{\partial^5}{\partial T_0 \partial x^4} w_0 \\
 &+ 2 \frac{\partial^2}{\partial T_1 \partial T_0} w_1 + 2 \frac{\partial^2}{\partial T_2 \partial T_0} w_0 + \frac{\partial^2}{\partial T_1^2} w_0 + 2\gamma \frac{\partial^2}{\partial T_1 \partial x} w_1 + 2\gamma \frac{\partial^2}{\partial T_2 \partial x} w_0 \\
 &+ \frac{1}{k_f^2} 4\alpha \pi (\gamma^2 - 1 - k_f^2 \pi^2) \sin(\pi x) \int_0^1 \left( \frac{\partial^2}{\partial T_0 \partial x} w_0 \right) \cos(\pi x) \, dx = 0
 \end{aligned} \tag{18}$$

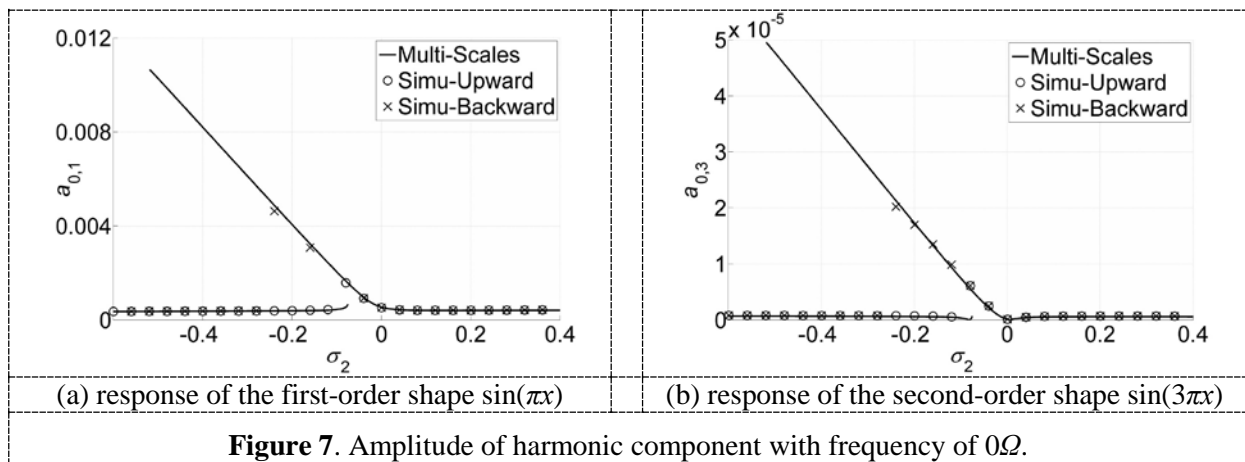
The general solution of Eq. (16) can be written as

$$w_0(x, T_0, T_1, T_2) = A_1(T_1, T_2)\Theta_1(x)e^{i\omega_1 T_0} + A_2(T_1, T_2)\Theta_2(x)e^{i\omega_2 T_0} + G(x)e^{i\Omega T_0} + cc \quad (19)$$

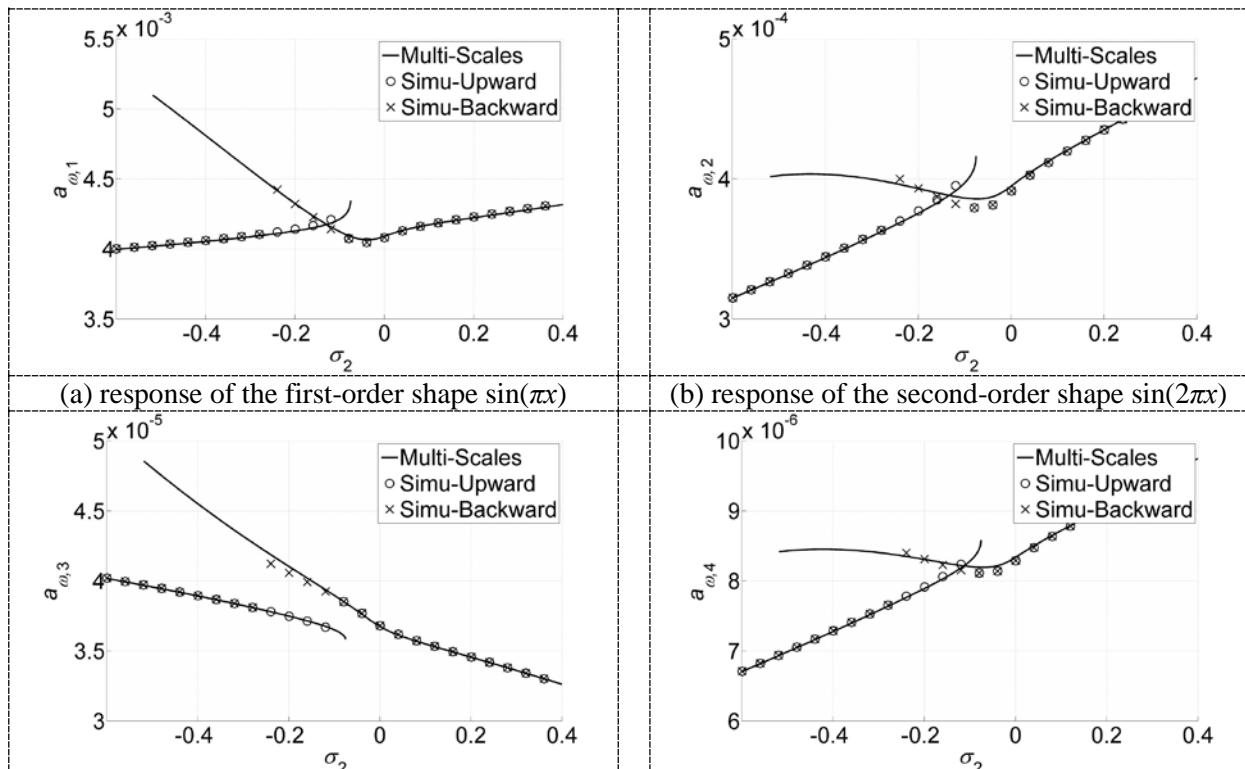
where  $cc$  is the complex conjugates of foregoing terms.  $A_1(T_1, T_2)$  and  $A_2(T_1, T_2)$  are undetermined functions and are solved by the solvable conditions.

#### 4.1. Harmonic component of $0\Omega$

The quadratic nonlinearity in the governing function yields a constant. It is included in the particular solution of Eq. (17). It occurs at the first and the third modal shapes. Solid lines are on behalf of analytically stable solutions. The up-bifurcations are nearly straight for this component has the relationship with  $a_1^2$  and  $a_2^2$ .



#### 4.2. Harmonic component of $1\Omega$



(c) response of the third-order shape $\sin(3\pi x)$	(d) response of the forth-order shape $\sin(4\pi x)$
--	--

**Figure 8.** Amplitude of harmonic component with frequency of  $1\Omega$ .

As the external frequency here is not equal to the first natural one, a harmonic response with  $1\Omega$  will occur. In figure 8, the responses at the first-four modal shapes are demonstrated. As can be seen from the figure, the curves are complicated. The upward branch is crossed with the backward one.

#### 4.3. Harmonic component of $2\Omega$

As shown in figure 9, solid lines present the analytical solutions, crosses and circles present simulations. The simulation results are calculated by 4-order Galerkin method. It clearly demonstrates that analytical solutions fit the numerical simulations very well. Moreover, nonlinearity of this harmonic response in figure 6 is also soft. Furthermore, the jumping range is the same as primary resonance. However, anti-resonance occurs in these harmonic responses. Their positive and negative properties determined by  $\sigma_2$  bring this special phenomenon.

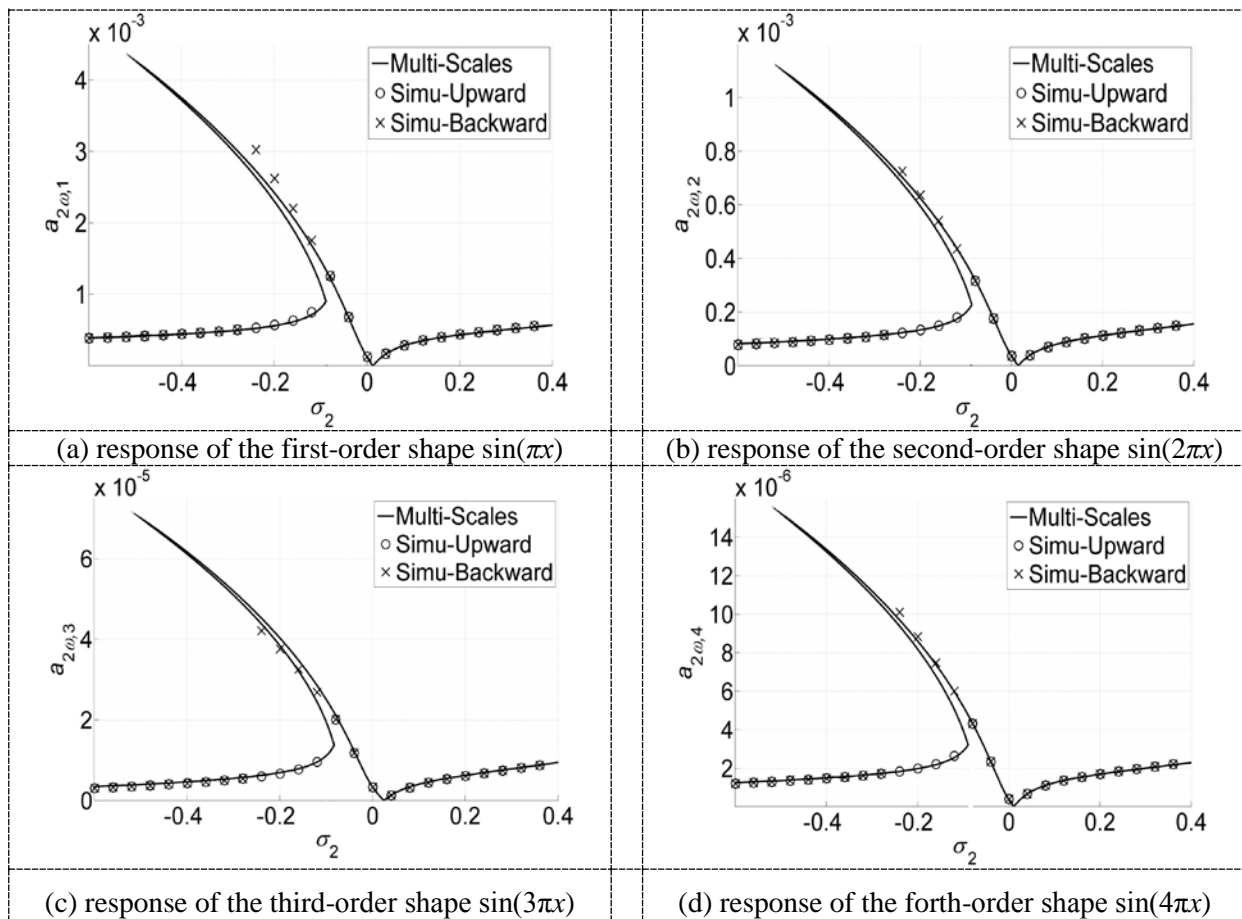


**Figure 9.** Amplitude of harmonic component with frequency of  $2\Omega$ .

#### 4.4. Harmonic component of natural modes

Figure 10 and 11 show the responses of the first-two natural modes. The coupling between the natural modes is weak. Response of the first mode at the first-order shape is sizable. The cubic nonlinearity plays the role of energy-transferring bridge.

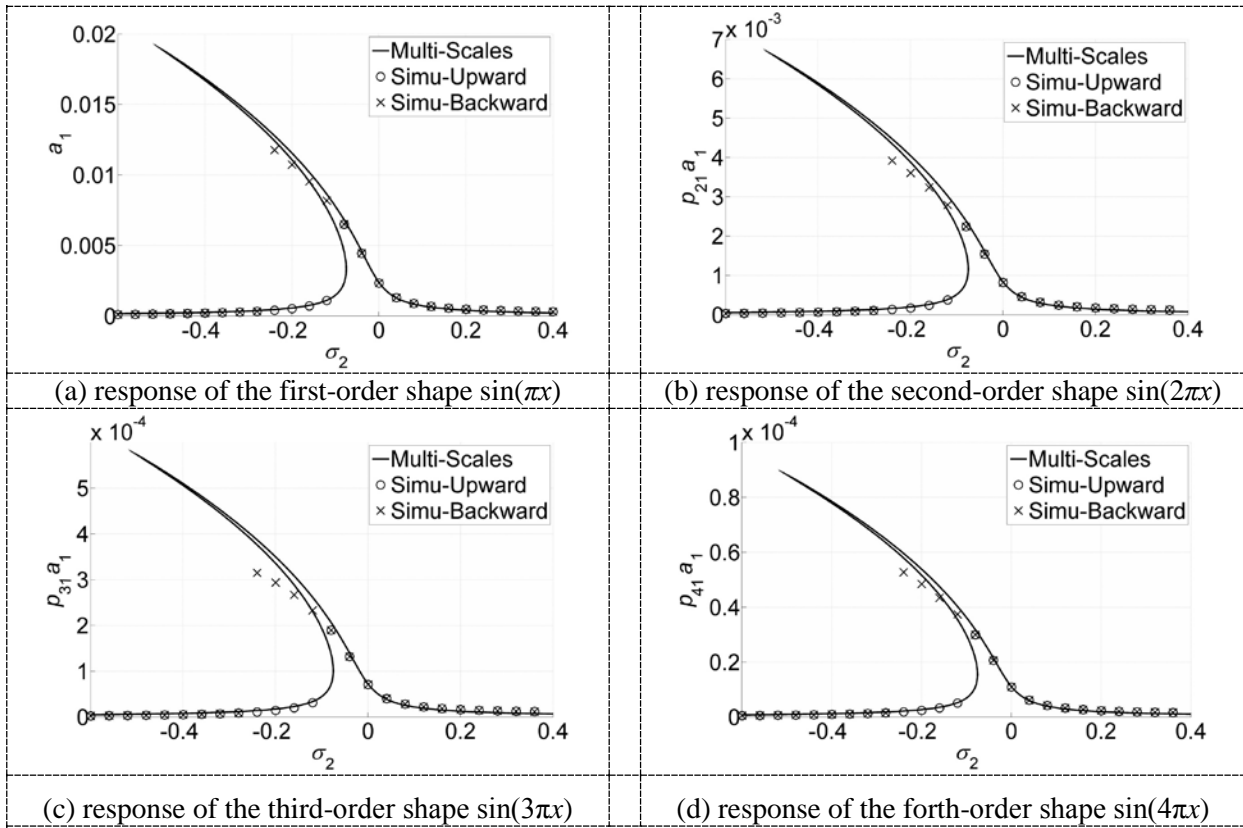


**Figure 10.** Amplitude of harmonic component with frequency of  $\omega_1$ .

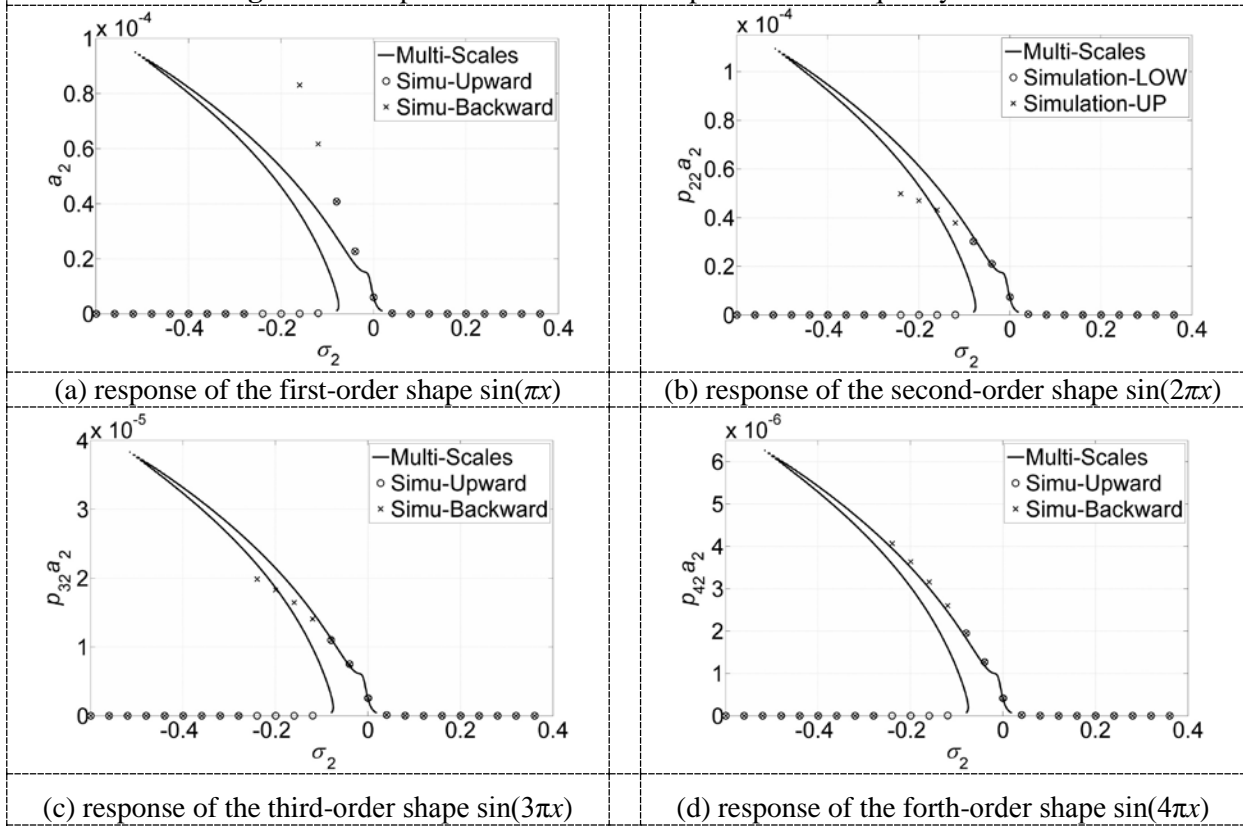


**Figure 11.** Amplitude of harmonic component with frequency of  $\omega_2$ .

4.5. Harmonic component of  $4\Omega$

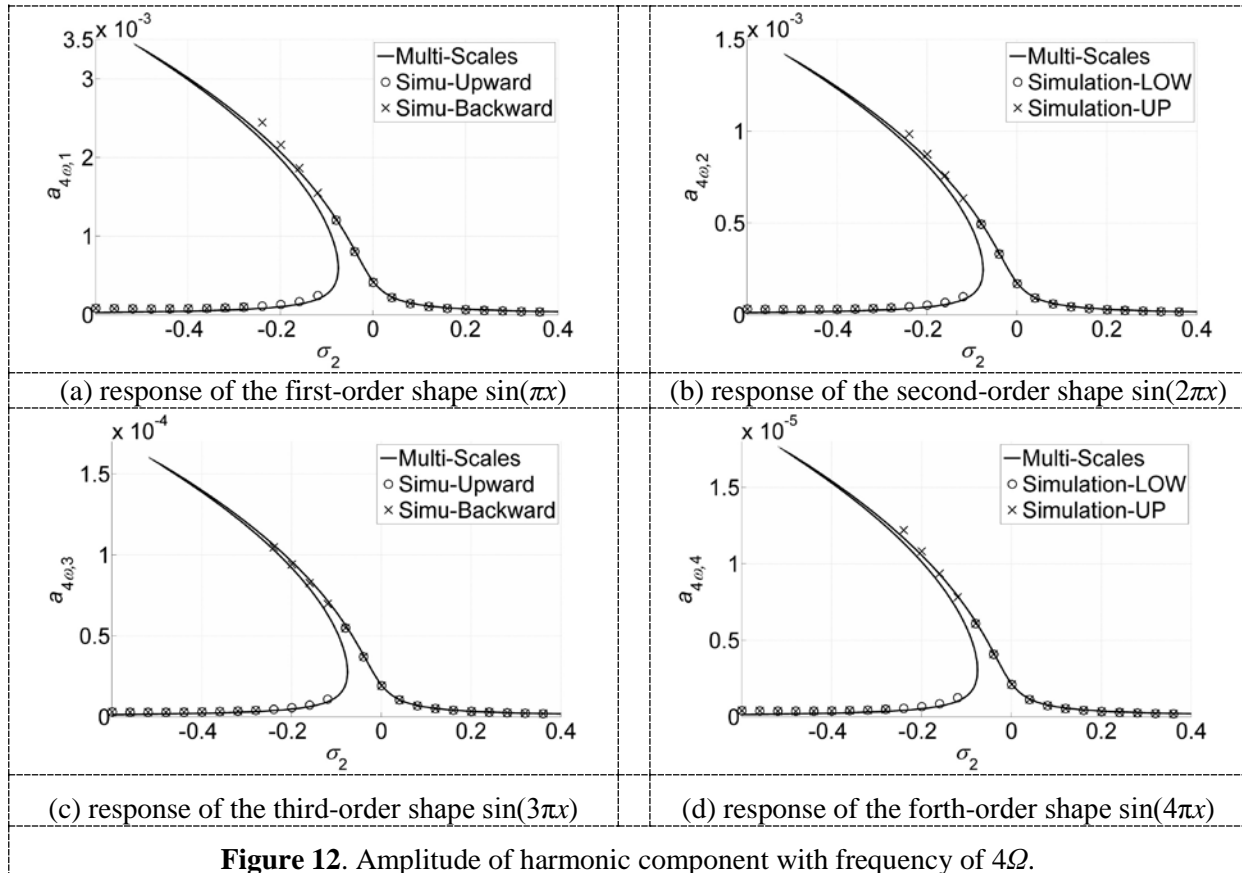
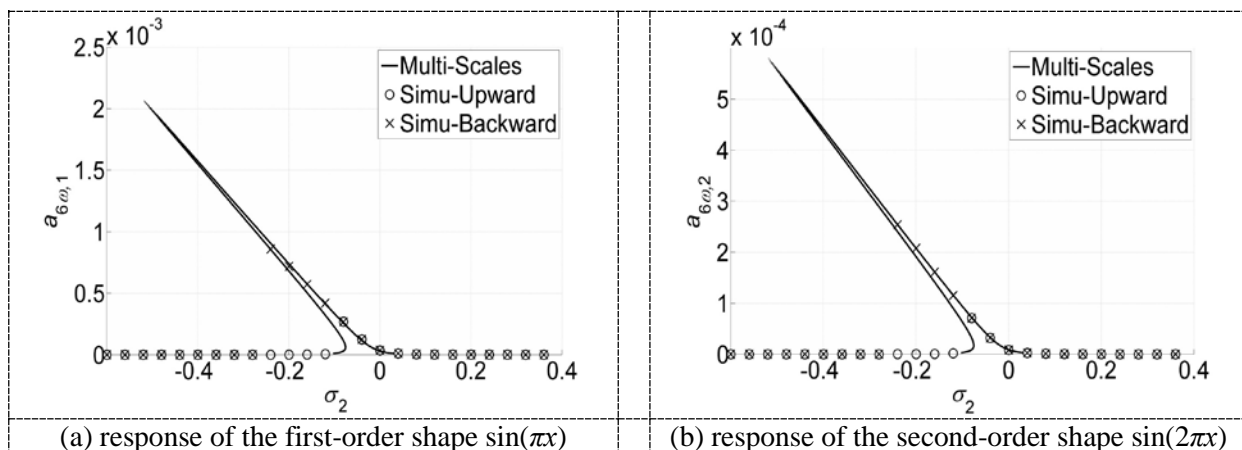
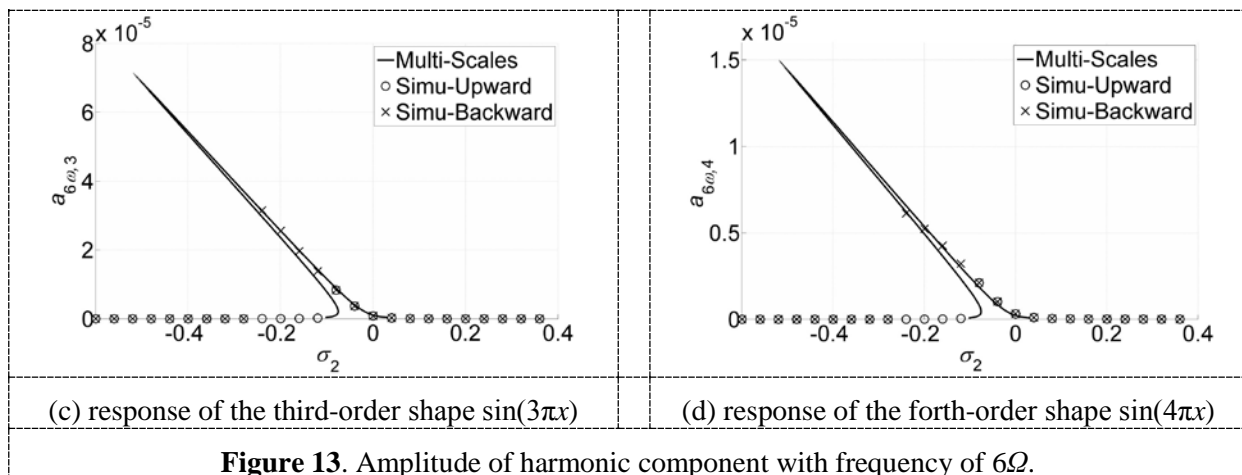


Figure 12 depicts the steady-state response amplitude-frequency curves of  $4\Omega$ . Solid line is in present of analytical results. It is coincide with simulations, the circles and crosses, very well. Besides, nonlinearity here is soft too. Jumping range is the same as the primary resonance.

4.6. Harmonic component of  $6\Omega$

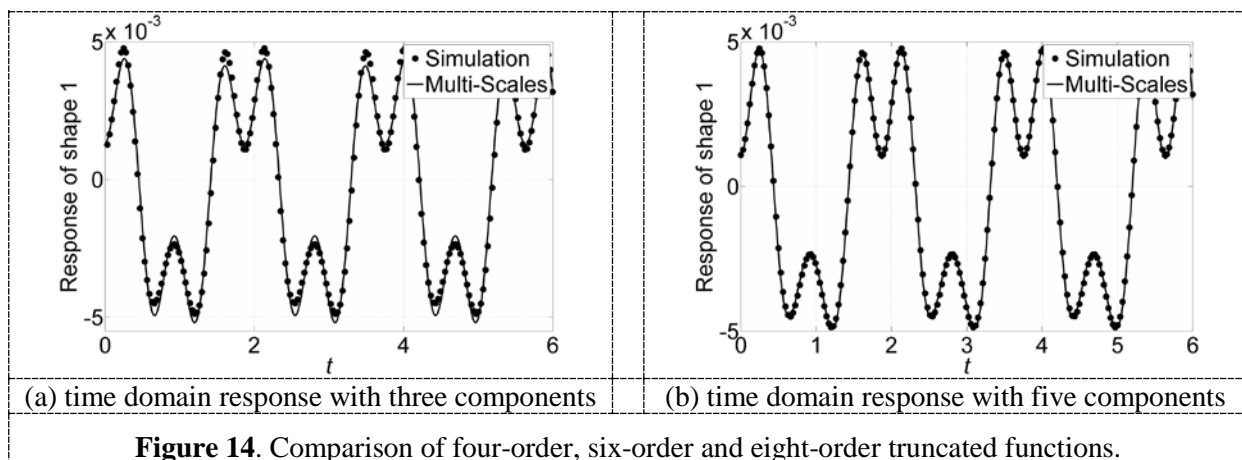
The amplitude of the resonance response is connected with the free vibration squared. The amplitude-frequency curves are shown in figure 13. The numerical results in figure 13 show that the analytical solutions are feasible and credible.





4.7. Convergence of the Galerkin truncated for super-harmonic resonance

To verify the convergence of the analytical solutions, time-domain responses with different numbers of harmonic components are compared with the simulations. As an example, the time-domain response of the first-order shape is shown in figure 14. The first one is composited with harmonic components of  $0\Omega$ ,  $1\Omega$  and  $\omega_1$ . Solid line presenting analytical solution is near to the simulations. But it is not accurate enough. The second one in figure 14 is composited with two more components. They are responses with frequency of  $2\Omega$  and  $4\Omega$ . It is anastomotic to the simulations. So the analytical method used in this study can obtain the key components in the responses.



5. Conclusions

In the present work, the steady-state response of axially moving beam in the supercritical speed range under the condition of 3:1 internal resonance is firstly studied. By using the Galerkin method, the partial-integral differential governing equation of the axially moving beam is truncated into 4 degrees of freedom ordinary differential equations. The analytical approximate solutions are derived by the multi-scale method. Moreover, the analytical results are confirmed by numerical simulations.

The approximate solutions discover some interesting phenomenon of the nonlinear forced vibration of the supercritically axially moving beam with the 3:1 internal resonance. Under the condition of 3:1 internal resonance and 1/3 super-harmonic resonance, response of the system is complicated and multi-component. The numerical results also find that the nonlinear character of the primary resonance is soft. Energy transmits from the first order mode two the second one. Therefore, the 3:1 internal resonance plays a coupling role. Moreover, the hysteresis phenomenon of super-harmonic resonance

portrays the change of amplitudes according to amplitude of excitation. Furthermore, some harmonic components are aroused under the condition of 1/3 super-harmonic resonance.

### Acknowledgments

The authors gratefully acknowledge the support of the State Key Program of the National Natural Science Foundation of China (No. 11232009) and the National Natural Science Foundation of China (No. 11372171, 11422214).

### References

- [1] Ozhan B B 2014 "Vibration and Stability Analysis of Axially Moving Beams with Variable Speed and Axial Force" *Int. J. Struct. Stab. Dy.* **14**
- [2] Yang X D and Zhang W 2014 "Nonlinear dynamics of axially moving beam with coupled longitudinal-transversal vibrations" *Nonlinear Dynam.* **78** 2547-2556
- [3] Yu W Q and Chen F Q 2013 "Multi-pulse homoclinic orbits and chaotic dynamics for an axially moving viscoelastic beam" *Arch. Appl. Mech.* **83** 647-660
- [4] Ding H and Zu J W 2014 "Steady-State Responses of Pulley-Belt Systems With a One-Way Clutch and Belt Bending Stiffness" *J. Vib. Acoust.* **136**
- [5] Riedel C H and Tan C A 2002 "Coupled, forced response of an axially moving strip with internal resonance" *Int. J. Nonlinear Mech.* **37** 101-116
- [6] Sze K Y, Chen S H and Huang J L 2005 "The incremental harmonic balance method for nonlinear vibration of axially moving beams" *J. Sound Vib.* **281** 611-626
- [7] Huang J L, et al. 2011 "Stability and bifurcation of an axially moving beam tuned to three-to-one internal resonances" *J. Sound Vib.* **330** 471-485
- [8] Ghayesh M H 2011 "Nonlinear forced dynamics of an axially moving viscoelastic beam with an internal resonance" *Int. J. Mech. Sci.* **53** 1022-1037
- [9] Ghayesh M H, Kazemirad S and Amabili M 2012 "Coupled longitudinal-transverse dynamics of an axially moving beam with an internal resonance" *Mech. Mach. Theory* **52** 18-34
- [10] Ghayesh M H and Amabili M 2013 "Nonlinear dynamics of an axially moving Timoshenko beam with an internal resonance" *Nonlinear Dynam.* **73** 39-52
- [11] Tang Y Q, Zhang D B and Gao J M 2016 "Parametric and internal resonance of axially accelerating viscoelastic beams with the recognition of longitudinally varying tensions" *Nonlinear Dynam.* **83** 401-418
- [12] Sahoo B, Panda L N and Pohit G 2016 "Combination, principal parametric and internal resonances of an accelerating beam under two frequency parametric excitation" *Int. J. Nonlinear Mech.* **78** 35-44
- [13] Wickert J A 1992 "Nonlinear Vibration of a Traveling Tensioned Beam" *Int. J. Nonlinear Mech.* **27** 503-517
- [14] Ding H and Chen L Q 2010 "Galerkin methods for natural frequencies of high-speed axially moving beams" *J. Sound Vib.* **329** 3484-3494
- [15] Ding H, et al. 2012 "Forced Vibrations of Supercritically Transporting Viscoelastic Beams" *J. Vib. Acoust.* **134**
- [16] Ghayesh M H, Kafiabad H A and Reid T 2012 "Sub- and super-critical nonlinear dynamics of a harmonically excited axially moving beam" *Int. J. Solids Struct.* **49** 227-243